Methodological Calibration of the Cell Transmission Model

Laura Muñoz, Xiaotian Sun, Dengfeng Sun, Gabriel Gomes, Roberto Horowitz

Abstract— A semi-automated method has been developed for calibrating the parameters of a modified version of Daganzo's Cell Transmission Model (CTM). A least-squares data fitting approach was applied to loop detector data to determine free-flow speeds, congestion-wave speeds, and jam densities for specified subsections of a freeway segment. Bottleneck capacities were estimated from measured mainline and on-ramp flows. The calibration method was tested on a 14-mile portion of Interstate 210 Westbound in southern California. The calibrated CTM was able to reproduce observed bottleneck locations and the approximate behavior of traffic congestion, yielding approximately 6%, or less, error in the predicted total travel time.

I. INTRODUCTION

Traffic congestion is a phenomenon frequently encountered on freeways. It has many detrimental effects, such as increasing driver delay and intensifying air pollution. Regulation, or metering, of on-ramp flows is often used as a method to help alleviate congestion on freeways. Accurate traffic models are desirable as both a basis for on-ramp metering control designs and as testbeds for proposed metering methods.

In an effort to find innovative solutions to the congestion problem, we are engaged in an ongoing collaboration between the California Department of Transportation, District 7, and PATH (Partners for Advanced Transit and Highways), with the goal of developing advanced freeway on-ramp metering control methods. One of the advanced control strategies proposed as part of this collaborative work employs the Cell Transmission Model (CTM) [1], [2] in determining optimal on-ramp metering rates for a freeway. The optimization method requires reasonably accurate estimates of the CTM parameters.

In this paper, we describe a methodology for tuning the CTM parameters to reproduce observed freeway traffic behavior. We have tested our calibration method on a 14-mile stretch of Interstate 210 Westbound (I-210W) in Pasadena, California, which typically endures heavy congestion during the weekday morning commute period. Our implementation of the CTM has been shown to capture the main features of the congestion evolution observed in the actual freeway, such as bottleneck formation, and the approximate temporal duration and spatial extent of the traffic congestion. Other examples of our recent work in CTM-based traffic modeling, traffic density estimation, and congestion mode estimation can be found in [3], [4], and [5].

The authors are with the Department of Mechanical Engineering, University of California at Berkeley, Berkeley, CA 94720-1740. Author for correspondence, R. Horowitz, email: `horowitz@me.berkeley.edu`.

II. MODIFIED CELL TRANSMISSION MODEL

The macroscopic cell-transmission traffic model was selected for this research due to its analytical simplicity and ability to reproduce important traffic behavioral phenomena, such as the backward propagation of congestion waves. The CTM has previously been validated for a single freeway link (with no on-ramps or off-ramps) using data from I-880 in California [6]. For this calibration study, we have used a modified CTM (MCTM), which is similar to that of [1], [2], except that it uses cell densities as state variables instead of cell occupancies[1], and accepts nonuniform cell lengths. Using cell densities instead of cell occupancies permits the CTM to accommodate uneven cell lengths, which leads to greater flexibility in partitioning the highway. The MCTM is subject to the same intercell connectivity restrictions as those described in [2].

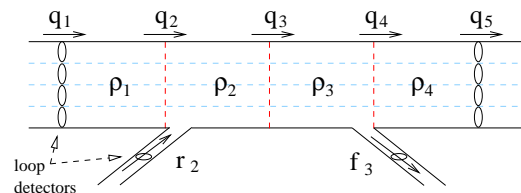In the modified CTM, a highway is partitioned into a series of cells. A 4-cell example is shown in Fig. 1. The

Fig. 1.   Highway segment divided into 4 cells.

traffic density in any cell i evolves according to conservation of vehicles:

$$\rho_i(k+1) = \rho_i(k) + \tfrac{T_s}{l_i}(q_{i,in}(k) - q_{i,out}(k)) \qquad (1)$$

where $q_{i,in}(k)$ and $q_{i,out}(k)$ are, respectively, the total flows, in vehicles per unit time, entering and leaving cell i during the kth time interval, $T_s[k,\ k+1)$, including flows along the mainline and the on- and off-ramps. k is the time index, T_s is the discrete time interval, l_i is the length of cell i, and $\rho_i(k)$ is the density, in vehicles per unit length of freeway, in cell i at time $k\,T_s$. The model parameters include v, w, Q_M, and ρ_J, which are depicted in the fundamental diagram of Fig. 2. They can be uniform over all cells or allowed to vary from cell to cell. The free-flow speed v is the average speed at which vehicles travel down the highway under uncongested (low density) conditions. w is the average speed at which congestion waves propagate upstream within congested (high density) regions of the highway. Q_M is the maximum flow rate, and ρ_J is the
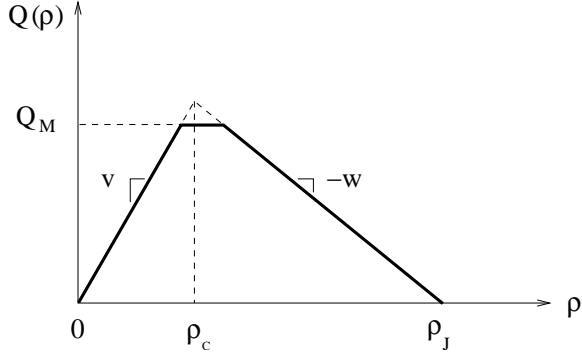
Fig. 2.   Flow as a function of density.

jam density. ρ_c, the critical density, is the density at which the free-flow curve $Q(\rho) = v\rho$ intersects the congestion curve $Q(\rho) = w(\rho_J - \rho)$. The *congestion status* of cell i is determined by comparing the cell density with the critical density: if $\rho_i < \rho_{c,i}$, the cell has free-flow status, otherwise $\rho_i \geq \rho_{c,i}$ and the cell is said to have congested status.

Three different types of intercell connection are allowed: simple connection, merge, and diverge.

Simple Connection: If two cells are connected to one another without any intervening on-ramps or off-ramps (for example, cells 2 and 3 in Fig. 1), then the cells are said to be simply connected. Let $i-1$ be the upstream cell and i be the downstream cell in the pair. As described in [2], $q_i(k)$, the flow entering cell i from the mainline, is determined by taking the minimum of two quantities:

$$q_i(k) = \min(S_{i-1}(k), R_i(k)), \qquad (2)$$

where $S_{i-1}(k) = \min(v_{i-1}\rho_{i-1}(k), Q_{M,i-1})$, is the maximum flow that can be *supplied* by cell $i-1$ under free-flow conditions, over the kth time interval, and $R_i(k) = \min(Q_{M,i}, w_i(\rho_J - \rho_i(k)))$, is the maximum flow that can be *received* by cell i under congested conditions, over the same time interval.

Merge: A merge connection corresponds to the case where an on-ramp intervenes between two cells (e.g. between cells 1 and 2 in Fig. 1). Assume that $r_{m,i+1}(k)$ is the measured demand at on-ramp $i+1$, and that $r_{i+1}(k)$ is the flow that actually enters the mainline from the on-ramp. We consider two cases, one where the downstream cell can accept both the supply flow from the upstream cell and the demand from the on-ramp, and one where the combined supply flow and on-ramp demand exceed the maximum receiving flow.

$$q_{i+1} = \begin{cases} S_i, & \text{if } S_i + r_{m,i+1} \leq R_{i+1} \\ \max(0, R_{i+1} - r_{m,i+1}), & \text{otherwise} \end{cases} \qquad (3)$$

In the latter case, i.e., when $S_i(k) + r_{m,i+1}(k) > R_{i+1}(k)$, we assume that the total flow entering the downstream cell is equal to $R_{i+1}(k)$, thus, in the event that $r_{m,i+1}(k)$ exceeds $R_{i+1}(k)$, a flow of $R_{i+1}(k)$ will be supplied by the on-ramp. In all other cases the on-ramp demand is given by

$r_{i+1}(k) = r_{m,i+1}(k)$. That is,

$$r_{i+1} = \begin{cases} r_{m,i+1}, & \text{if } S_i + r_{m,i+1} \leq R_{i+1} \\ R_{i+1} - q_{i+1}, & \text{otherwise} \end{cases} \qquad (4)$$

For brevity, the time index k has been suppressed in Eqs. (3) and (4).

Diverge: If the outflow from a cell is split between the downstream mainline region and an off-ramp, a diverge connection is warranted; an example is shown between cells 3 and 4 in Fig. 1. We assume that each off-ramp has unlimited capacity. Then the diverge law of [2] simplifies to

$$q_{i,out}(k) = \min\left(S_i(k), \frac{R_{i+1}(k)}{1-\beta_i(k)}\right) \qquad (5)$$

where $q_{i,out}(k) = q_{i+1}(k) + f_i(k)$ is the total flow exiting cell i, and $f_i(k)$ is the off-ramp flow. The flow entering the downstream cell is then given by $(1 - \beta_i(k))q_{i,out}(k)$, and the flow exiting through the off-ramp is $\beta_i(k)q_{i,out}(k)$, where $\beta_i(k)$ is the *split ratio* for off-ramp i, i.e., the fraction of vehicles leaving cell i which exits through the off ramp during the kth time interval.

The modified CTM consists of flow conservation, Eq. (1), for each cell, along with the flow specifications, Eqs. (2)–(5). The aforementioned equations are the density-based equivalents of those described in [2]. The state variable is $\boldsymbol{\rho} = [\rho_1 \ldots \rho_N]^T$ for a freeway partitioned into N cells, and the model inputs are the demands at each on-ramp and at the mainline entrance to the freeway. Flows at the upstream and downstream mainline boundaries of the freeway are determined from Eqs. (3), (4), (5), treating the mainline entrance as an on-ramp, and the mainline exit as an off-ramp with $\beta_N = 1$.

III. CALIBRATION METHODOLOGY

A. Freeway Representation

We have divided the 14-mile I-210W test segment into 41 cells, as shown in Fig. 3. The traffic flow direction is in order of increasing cell index, i.e., left to right, starting at the top of the figure. The cell index is located in the center of each cell. The uppermost row of numbers above the cells is the cell length (in feet). The second row of numbers gives the number of mixed-flow lanes (4 to 6) in each cell. Vertical red (or gray in a gray-scale printout) bars mark the locations of the mainline loop detectors, and the postmile of the detector (e.g. 39.159) is listed above the detector marker. On- and off-ramps are depicted as numbered arrows. Associated street names are given for each set of ramps. A single high-occupancy vehicle (HOV) lane runs parallel to the leftmost mainline lane on this segment of I-210W. Each of the six HOV-lane gates is indicated by a horizontal blue (or gray) bar. In the real freeway, vehicles are only allowed to enter and leave the HOV lane at the gate locations. In our implementation, HOV/mixed-flow lane interaction is only partially modeled, as explained in Sec. III-B.
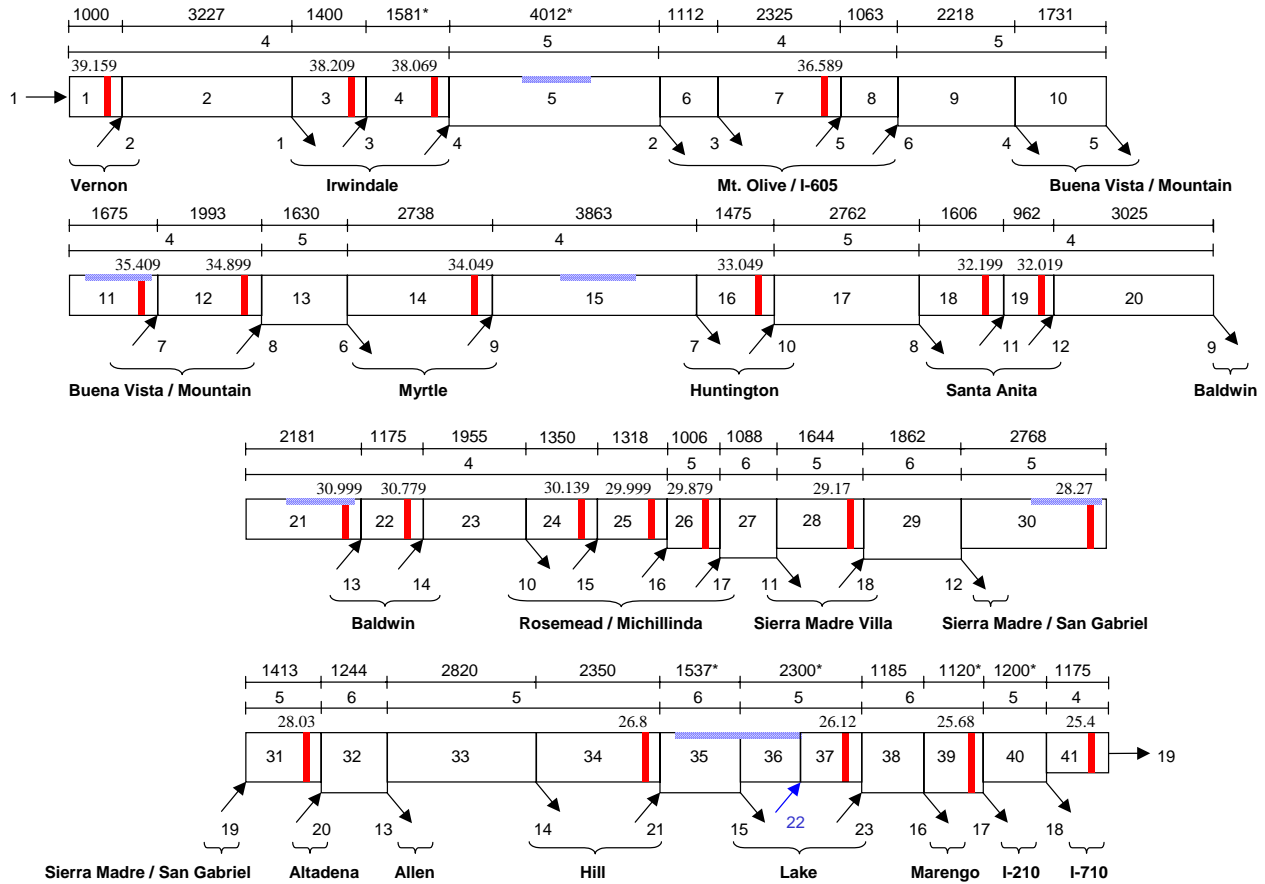
Fig. 3.   Cell partition of I-210W testbed.

One requirement of the MCTM is that the cell lengths must be longer than the free-flow travel distance, i.e., $v_i T_s \leq l_i$ for cell i, where l_i is the cell length and T_s is the time step. In our default partitioning method, we put cell boundaries immediately upstream of on-ramps and immediately downstream of off-ramps; however, for our chosen time step of 10 sec., and a typical free flow speed of 63 mph, three of the cells were found to be shorter than the minimum allowed cell length of 924 ft. We increased the length of these cells by borrowing length from their respective downstream cells, and these adjusted cell lengths are shown with asterisks in Fig. 3.

B. Demand and Split Ratio Reconstruction

In this study, we have been working with two main sources of data: loop detector data obtained from the Performance Measurement System (PeMS) [7], and a set of manually-counted on-ramp and off-ramp volumes provided to us by the Caltrans District 7 Traffic Operations Group. The PeMS-derived data used in this study includes the flow (veh/hr or vph) at each detector, updated every 30 sec., and the density (veh/mi or vpm) at each mainline detector, which is available in 5-min. averages. Speed (mph) is determined from the relationship *flow = density × speed*.

One problem we face in calibrating traffic models is that our data sources, collectively, do not provide us with a complete data set (which would include flows and densities for each mainline and HOV-lane detector, along with flows measured at each of the ramps, over the entire morning period) for any single day of data collection. Missing measurements are mainly caused by malfunctioning detectors, or problems affecting the transmission of loop data, in the case of the PeMS data sets. For the manually-counted data, on any given day there are some ramps for which no volumes have been recorded.

For our model, a complete demand data set consists of the measured flow at the upstream mainline (Vernon) boundary, along with the measured flows at each on-ramp, over the period 5AM–12PM for a selected day. If PeMS data is faulty or absent at a particular on-ramp, our first preference is to substitute manual counts, if they are available for that day. If there is no hand-counted data for the chosen day, we substitute a historical average of the manually-counted flows for that on-ramp.

Our procedure for estimating the MCTM split ratios is to compute, for each off-ramp, the ratio of the measured off-ramp flow to the total measured flow (mainline plus off-ramp) exiting the diverge junction. Since we have access to only a limited amount of accurate off-ramp data, we are currently using historically averaged split ratios in our MCTM simulations.

To estimate the extent to which the HOV lane affects the mixed-flow lanes, we computed the flow difference (upstream minus downstream flow) in the HOV lane across each of the HOV gates, and determined that this net flow is relatively large (in the range of 500–1500 vph) and of consistent sign (positive) only at the farthest downstream gate, near Lake Ave. For this study, we approximated this effect by creating an additional on-ramp (no. 22), computing the net flow rate across the Lake HOV gate, and inserting this flow into the mixed-flow lanes through the new ramp. The remaining HOV gates were not modeled.

C. Calibration Procedure

The main steps of the calibration procedure are as follows:

1) Free-flow Parameter Calibration: The free-flow traffic velocities, v_i, are determined by performing a least-squares fit on the flow vs. density data over the period 5:00–6:00AM. For the I-210 section, traffic typically flows freely during this period. For the jth detector, v_j is the solution, in the least-squares sense, to the equation $\phi_j v_j = Y_j$, where $\phi_j = [\rho_{d_j}(k_{5:00}) \ldots \rho_{d_j}(k_{6:00})]^T$ and $Y_j = [q_{d_j}(k_{5:00}) \ldots q_{d_j}(k_{6:00})]^T$ are the measured densities and flows over the specified time interval. If no data is available, or the data is of poor quality, a default value of 60 mph is used. The free-flow speed v_j is assigned to the cell containing detector j, and free-flow speeds are computed for non-detector cells by linear interpolation. The resulting v_i are typically in the range of 60–65 mph.

2) Bottleneck Identification: Bottleneck locations are identified by examining contour plots of the measured traffic densities and/or speeds, and determining the locations of fixed spatial boundaries which divide the freeway into an upstream congested region and a downstream free-flow region. For example, in the top plot of Fig. 5, a bottleneck was observed to form between the detectors at 33.049 and 32.199 during the 6:00 time slice.

3) Non-Bottleneck Capacity Selection: Currently, a set of nominal $Q_{M,i}$ are assigned to the cells that are not located at bottlenecks. It is expected that $Q_{M,i}$, which represents the maximum flow that can possibly enter or exit cell i, will typically not be achieved (and hence not be observed) in the real system. Thus, it is not advisable to set $Q_{M,j}$ equal to the maximum observed flow at each detector-equipped cell, since this will most likely result in underestimating the true capacity of the freeway. In general, the nominal $Q_{M,i}$ must be chosen to be larger than the maximum observed flows (usually ≥ 2000 veh/hr per lane (vphpl)) in each region of the highway, in order to avoid inducing unwanted bottlenecks in the simulation.

4) Bottleneck Capacity Determination: Consider the scenario suggested by Fig. 4: an active bottleneck exists between cell 1 and cell 2, hence the upstream cell is congested, while the downstream cell remains in free-flow status. We assume that the inflow into cell 1 is $w_1(\rho_{J,1} - \rho_1(k))$, the total inflow to cell 2 is $Q_{M,2}$, the total outflow from cell
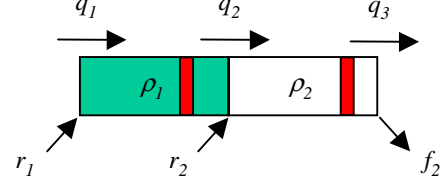
Fig. 4. An active bottleneck: the upstream cell (1) is congested, while the downstream cell (2) is in free-flow mode. Vertical red bars indicate detectors.

2 is $v_2\rho_2(k)$, and that the second case in the maximum of Eq. (3) holds, that is, the measured demand $r_{m,2}$ is not larger than the amount of flow that cell 2 can accommodate. In this situation, the MCTM equations for these two cells reduce to a linear system. The density dynamics are given by:

$$\rho_1(k+1) = \rho_1(k) + \frac{T_s}{l_1}(w_1(\rho_{J,1} - \rho_1(k)) - Q_{M,2} + r_2(k)) \qquad (6)$$

$$\rho_2(k+1) = \rho_2(k) + \frac{T_s}{l_2}(Q_{M,2} - v_2\rho_2(k)) \qquad (7)$$

The total flow entering cell 2 is $Q_{M,2} = q_2 + r_2$, where q_2 is the flow entering from the mainline. Since both q_2 and r_2 are measurable, these quantities are used to estimate the bottleneck flow rate, specifically, $\hat{Q}_{M,2} = \text{mean}_{k \in K_M}(q_2(k) + r_2(k))$. K_M corresponds to the half-hour time interval ending at $\arg\max(q_2(k) + r_2(k))$. If, for a selected day, the q_2 or r_2 data are considered faulty, $Q_{M,2}$ is estimated using historically averaged q_2 or r_2 data sets.

5) Congestion Parameter Calibration: w_i and $\rho_{J,i}$ are estimated by performing a constrained least-squares fit on the flow vs. density measurements. First, the critical density is estimated for each detector; $\hat{\rho}_{c,j} = \max_k(q_{d_j}(k))/v_j$. The $(\rho_{d_j}(k), q_{d_j}(k))$ data is sorted so that only congested pairs are used in the estimation. Let $\kappa = \{k_1 \ldots k_{N_c}\}$ denote the set of all k for which $\rho_{d_j}(k) > \hat{\rho}_{c,j}$. $[w_j \ w_j\rho_{J,j}]^T$ is the solution, in the least-squares sense, to

$$\phi_j \begin{bmatrix} w_j \\ w_j\rho_{J,j} \end{bmatrix} = Y_j \qquad (8)$$

where

$$\phi_j^T = \begin{bmatrix} -\rho_{d_j}(k_1) & \ldots & -\rho_{d_j}(k_{N_c}) \\ 1 & \ldots & 1 \end{bmatrix}$$

and

$$Y_j = \begin{bmatrix} q_{d_j}(k_1) + \frac{l_j}{T_s}\Delta\rho_{d_j}(k_1) \\ \vdots \\ q_{d_j}(k_{N_c}) + \frac{l_j}{T_s}\Delta\rho_{d_j}(k_{N_c}) \end{bmatrix},$$

where $\Delta\rho_{d_j}(k) = \rho_{d_j}(k+1) - \rho_{d_j}(k)$. Note that Eq. (8), which is linear in the unknown parameters $[w_j \ w_j\rho_{J,j}]^T$, is a rewriting of the congested case of the MCTM, where q_{d_j} is taken as a measurement of the flow exiting the cell containing detector j. In the congested case, inter-cellular flow is determined by the downstream density in each pair

Fig. 5. Contour plots of 15-minute average measured (top) and simulated (bottom) densities (vpmpl) on Nov. 28, 2001.

Measured Density (time in hrs vs. postmile)

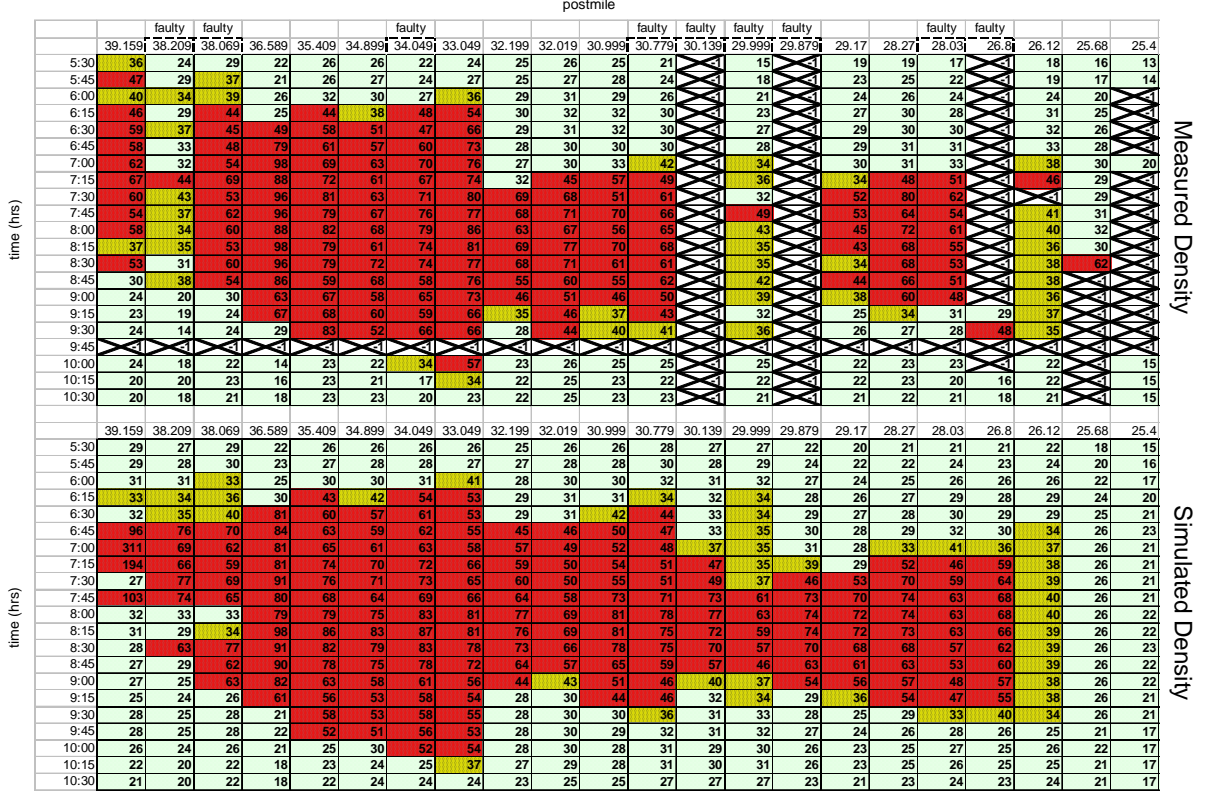| time	39.159	38.209 faulty	38.069 faulty	36.589	35.409	34.899	34.049 faulty	33.049	32.199	32.019	30.999	30.779 faulty	30.139 faulty	29.999 faulty	29.879 faulty	29.17	28.27	28.03 faulty	26.8 faulty	26.12	25.68	25.4
5:30	36	24	29	22	26	26	22	24	25	26	25	21	✕	15	✕	19	19	17	✕	18	16	13
5:45	47	29	37	21	26	27	24	27	25	27	28	24	✕	18	✕	23	25	22	✕	19	17	14
6:00	40	34	39	26	32	30	27	36	29	31	29	26	✕	21	✕	24	26	24	✕	24	20	✕
6:15	46	29	44	25	44	38	48	54	30	32	32	30	✕	23	✕	27	30	28	✕	31	25	✕
6:30	59	37	45	49	58	51	47	66	29	31	32	30	✕	27	✕	29	30	30	✕	32	26	✕
6:45	58	33	48	79	61	57	60	73	28	30	30	30	✕	28	✕	29	31	31	✕	33	28	✕
7:00	62	32	54	98	69	63	70	76	27	30	33	42	✕	34	✕	30	31	33	✕	38	30	20
7:15	67	44	69	88	72	61	67	74	32	45	57	49	✕	36	✕	34	48	51	✕	46	29	✕
7:30	60	43	53	96	81	63	71	80	69	68	51	61	✕	32	✕	52	80	62	✕		29	✕
7:45	54	37	62	96	79	67	76	77	68	71	70	66	✕	49	✕	53	64	54	✕	41	31	✕
8:00	58	34	60	88	82	68	79	86	63	67	56	65	✕	43	✕	45	72	61	✕	40	32	✕
8:15	37	35	53	98	79	61	74	81	69	77	70	68	✕	35	✕	43	68	55	✕	36	30	✕
8:30	53	31	60	96	79	72	74	77	68	71	61	61	✕	35	✕	34	68	53	✕	38	62	✕
8:45	30	38	54	86	59	68	58	76	55	60	55	62	✕	42	✕	44	66	51	✕	38	✕	✕
9:00	24	20	30	63	67	58	65	73	46	51	46	50	✕	39	✕	38	60	48	✕	36	✕	✕
9:15	23	19	24	67	68	60	59	66	35	46	37	43	✕	32	✕	25	34	31	29	37	✕	✕
9:30	24	14	24	29	83	52	66	66	28	44	40	41	✕	36	✕	26	27	28	48	35	✕	✕
9:45	✕	✕	✕	✕	✕	✕	✕	✕	✕	✕	✕	✕	✕	✕	✕	✕	✕	✕	✕	✕	✕	✕
10:00	24	18	22	14	23	22	34	57	23	26	25	25	✕	25	✕	22	23	23	✕	22	✕	15
10:15	20	20	23	16	23	21	17	34	22	25	23	22	✕	22	✕	22	23	20	16	22	✕	15
10:30	20	18	21	18	23	23	20	23	22	25	23	23	✕	21	✕	21	22	21	18	21	✕	15

Simulated Density (time in hrs vs. postmile)

time	39.159	38.209	38.069	36.589	35.409	34.899	34.049	33.049	32.199	32.019	30.999	30.779	30.139	29.999	29.879	29.17	28.27	28.03	26.8	26.12	25.68	25.4
5:30	29	27	29	22	26	26	26	26	25	26	26	28	27	27	22	20	21	21	21	22	18	15
5:45	29	28	30	23	27	28	28	27	27	28	28	30	28	29	24	22	22	24	23	24	20	16
6:00	31	31	33	25	30	30	31	41	28	30	30	32	31	32	27	24	25	26	26	26	22	17
6:15	33	34	36	30	43	42	54	53	29	31	31	34	32	34	28	26	27	29	28	29	24	20
6:30	32	35	40	60	57	61	53	58	29	31	42	44	33	34	29	27	28	30	29	29	25	21
6:45	96	76	70	84	63	59	62	55	45	46	50	47	33	35	30	28	29	32	30	34	26	23
7:00	311	69	62	81	65	61	63	58	57	49	52	48	37	35	31	28	33	41	36	37	26	21
7:15	194	66	59	91	74	70	72	66	59	50	54	51	47	35	39	29	52	46	59	38	26	21
7:30	27	77	69	91	76	71	73	65	60	50	55	51	49	37	46	53	70	59	64	39	26	21
7:45	103	74	65	80	68	64	69	66	64	58	73	71	73	61	73	70	74	63	68	40	26	21
8:00	32	33	33	79	79	75	83	81	77	69	81	78	77	63	74	72	74	63	68	40	26	22
8:15	31	29	34	98	86	83	87	81	76	69	81	75	72	59	74	72	73	63	66	39	26	22
8:30	28	63	77	91	82	79	83	78	73	66	78	75	70	57	70	68	68	57	62	39	26	23
8:45	27	29	62	90	78	75	78	72	64	57	65	59	57	46	63	61	63	53	60	39	26	22
9:00	27	25	63	82	63	58	61	56	44	43	51	46	40	37	54	56	57	48	57	38	26	22
9:15	25	24	26	61	56	53	58	54	28	30	44	46	32	34	29	36	54	47	55	38	26	21
9:30	28	25	28	21	58	53	58	55	28	30	30	36	31	33	28	25	29	33	40	34	26	21
9:45	28	25	28	22	52	51	56	53	28	30	29	32	31	32	27	24	26	28	26	25	21	17
10:00	26	24	26	21	25	30	52	54	28	30	28	31	29	30	26	23	25	27	25	26	22	17
10:15	22	20	22	18	23	24	25	37	27	29	28	31	30	31	26	23	25	26	25	25	21	17
10:30	21	20	22	18	22	24	24	24	23	25	25	27	27	27	23	21	23	24	23	24	21	17

of cells; for example, the congested-mode equation for cell 1 in Fig. 4 is

$$\rho_1(k+1) = \rho_1(k) + \frac{T_s}{l_1}\left(w_1(\rho_{J,1} - \rho_1(k)) - w_2(\rho_{J,2} - \rho_2(k)) + r_2(k)\right) \quad (9)$$

The least-squares solution is subject to the constraint

$$\hat{Q}_{M,j} \le \frac{v_j\, w_j\, \rho_{J,j}}{v_j + w_j} \quad (10)$$

The constraint is included to prevent the solution $[w_j \ \ w_j\rho_{J,j}]^T$ from limiting the maximum possible flow in cell j below the $\hat{Q}_{M,j}$ identified in step III-C.4. As an example, referring to Fig. 1, suppose that the flow associated with a density ρ is given by $Q(\rho)$. It can be shown that for a given set of $(v, Q_M, w, \rho_J) > 0$, the maximum possible flow rate is $\min(Q_M, \frac{vw\rho_J}{v+w})$. Thus, the constraint prevents the lines $Q(\rho) = v\rho$ and $Q(\rho) = w(\rho_J - \rho)$ from intersecting below the $Q(\rho) = Q_M$ line. Since Q_M is intended to represent the maximum permissible flow in a cell, this constraint ensures that the maximum flow rate is achievable by the model. Currently, only values of w_j that fall within a range that is considered physically reasonable, $10 \le w_j \le 20$ mph, are retained. If Eqs. (8) and (10) fail to produce a solution in the acceptable range for a particular detector cell n, this cell is assigned the w_j of the nearest downstream neighbor with a w inside the range. The corresponding $\rho_{J,n}$ is found by solving the equality case of constraint (10). w_i and $\rho_{J,i}$ are then determined for non-detector cells through linear interpolation.

6) Time-Varying Parameter Adjustments: If necessary, we can apply temporary parameter changes (e.g. reduction of $Q_{M,i}$ in a region) to reproduce the effect of an incident. Also, by reducing w_i in the mid-morning time range, when the traffic is still congested but beginning its recovery back to the free-flow mode, we can approximate the effect of flow-density hysteresis.

IV. RESULTS

Figure 5 shows contour plots for the measured (top) and simulated (bottom) densities for a particular day (Wednesday, Nov. 28, 2001) in the I-210 testbed. The numbers inside the shaded cells are traffic densities, in vehicles per mile per lane (vpmpl). Free-flow densities (0–33 vpmpl) are shown as green (or white in a gray-scale printout). Mid-range congestion (33–43 vpmpl) is shaded yellow (medium gray). Red (dark gray) indicates heavy congestion (43 vpmpl or greater). Traffic is flowing from left to right in these plots, and the time, in 15-minute intervals, is given in the leftmost column. The time range is 5:30–10:30AM. Loop detector outages are indicated by crossed-out boxes in the measured-data contour plot. Loop detectors which were suspected to be faulty for the whole day have their postmile labels surrounded by a dashed box at the top of the measured-data plot.

The MCTM parameters used in this simulation are plotted in Fig. 6, along with those estimated for two other weekdays. The nominal $Q_{M,i}$ was chosen as 2300 vphpl for the 5 cells farthest upstream, and 2100 vphpl for the remaining
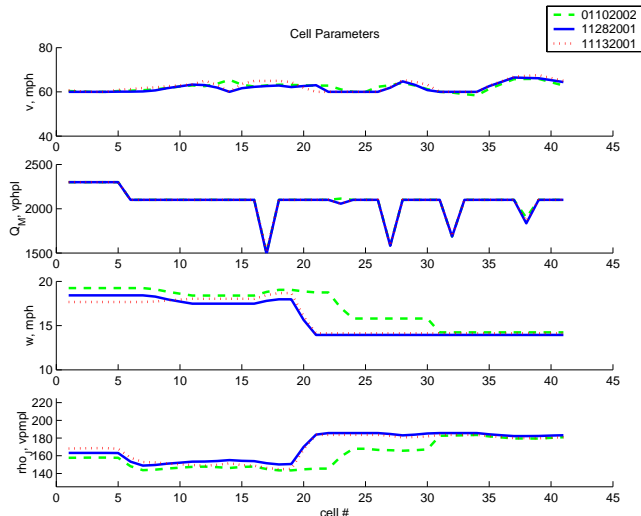
Fig. 6. MCTM parameters used for Nov. 13, 2001, Nov. 28, 2001 and Jan. 10, 2002 simulations.

cells. For the Jan. 10, 2002 parameters, it can be seen that w_i and $\rho_{J,i}$ differ from those of the other two days, in the region between cells 20 and 30. This difference was caused by the lack of good data in this region, including bottlenecks at postmiles 30.779 and 28.879, on Nov. 11 and 28, 2001. For these two days, historically averaged data were used to estimate the $Q_{M,i}$, and the w_i and $\rho_{J,i}$ were determined from the interpolation methods described in Sec. III, in the region of faulty data. A larger amount of good data was available in this region on Jan. 10, 2002, which produced different parameter estimates for this day.

To evaluate the performance of the simulation, we define the Total Travel Time (TTT):

$$TTT = T_s \sum_{k=k_{5:00}}^{k_{11:45}} \sum_{i \in C_d} l_i \rho_i(k)$$

Here, C_d is the set of cells which had problem-free mainline detectors over each of the examined days. C_d excludes detectors at postmiles 38.209, 38.069, 34.049, 30.779, 30.139, 29.999, 29.879, 28.030, and 26.800. Although it functions properly, the detector at 39.159 is also excluded, since the MCTM boundary condition prevents it from accurately reproducing congestion that (in the real system) spills upstream outside of the simulated region. Results for TTT are summarized in Table I.

From Fig. 5 and Table I, it can be seen that the MCTM reproduces the observed bottlenecks and the approximate duration and spatial extent of the congestion upstream of each bottleneck, and predicts the total travel time with approximately 6% error, or less.

V. Conclusions and Future Work

A procedure for calibrating the modified CTM has been presented in this paper. The calibrated model has been tested on a section of I-210W in southern CA, and has been shown to reproduce the main features of the observed traffic

Date	Meas.	Sim.	% Err.
Nov. 13, 2001	4249	3982	-6.3
Nov. 28, 2001	4375	4409	0.8
Jan. 10, 2002	3871	3863	-0.2
mean	4165	4085	-1.9
std. dev.	262	287	3.8

congestion on the freeway, such as approximate location of bottlenecks and duration and spatial extent of congestion. In addition, the model accurately predicts the total travel time in the freeway.

A main benefit of this calibration method is that it provides a well-defined, automatable procedure for estimating free-flow speeds, congestion parameters, and bottleneck capacities for the MCTM from loop-detector data. In the next stage of our work, we intend to develop a fully-automated parameter estimator. The quantities which still remain to be determined automatically include the bottleneck locations, the cell capacities away from the bottleneck locations, and the locations of faulty loop detectors. Our research team has already designed an estimator [4], [5] that determines the congestion status of each portion of the freeway. This estimator can be used to automatically locate bottlenecks, i.e., the boundaries separating upstream congested regions from downstream free-flow regions. Algorithms such as that of [8], can be employed to detect data errors and impute missing data values. Combining these approaches with our existing calibration methodology will lead to a fully-automated algorithm, which will be used to provide parameter values for model-based on-ramp metering control strategies.

References

[1] Carlos F. Daganzo. The Cell Transmission Model: A Dynamic Representation of Highway Traffic Consistent with the Hydrodynamic Theory. *Transportation Research - B*, 28(4):269–287, 1994.

[2] Carlos F. Daganzo. The Cell Transmission Model, Part II: Network Traffic. *Transportation Research - B*, 29(2):79–93, 1995.

[3] Laura Muñoz, Xiaotian Sun, Roberto Horowitz, and Luis Alvarez. Traffic Density Estimation with the Cell Transmission Model. In *2003 American Control Conference Proceedings*, pages 3750–3755, Denver, CO, June 4–6 2003.

[4] Xiaotian Sun, Laura Muñoz, and Roberto Horowitz. Highway Traffic State Estimation Using Improved Mixture Kalman Filters for Effective Ramp Metering Control. In *Proceedings of the 42nd IEEE Conference on Decision and Control*, pages 6333–6338, Maui, Hawaii, December 9–12 2003.

[5] Xiaotian Sun, Laura Muñoz, and Roberto Horowitz. Mixture Kalman Filter Based Highway Congestion Mode and Vehicle Density Estimator and its Application. In *2004 American Control Conference Proceedings*, Boston, Massachusetts, June 30 – July 2 2004. To appear.

[6] Wei-Hua Lin and Dike Ahanotu. Validating the Basic Cell Transmission Model on a Single Freeway Link. PATH Technical Note 95-3, Institute of Transportation Studies, University of California at Berkeley, 1994.

[7] Freeway Performance Measurement Project. `http://pems.eecs.berkeley.edu/`.

[8] Chao Chen, Jaimyoung Kwon, Alexander Skabardonis, and Pravin Varaiya. Detecting Errors and Imputing Missing Data for Single Loop Surveillance Systems. In *Transportation Research Board 82nd Annual Meeting*, Washington, D.C., August 2002.